Cone Dystrophy with Supernormal Rod Response Is Strictly Associated with Mutations in *KCNV2*

Bernd Wissinger,[1] *Susann Dangel,*[1] *Herbert Jägle,*[2] *Lars Hansen,*[3] *Britta Baumann,*[1] *Günther Rudolph,*[4] *Christiane Wolf,*[1] *Michael Bonin,*[5] *Katja Koeppen,*[1] *Thomas Ladewig,*[1] *Susanne Kohl,*[1] *Eberhart Zrenner,*[2] *and Thomas Rosenberg*[6]

Purpose. Cone dystrophy with supernormal rod response (CDSRR) is a retinal disorder characterized by reduced visual acuity, color vision defects, and specific alterations of ERG responses that feature elevated scotopic b-wave amplitudes at high luminance intensities. Mutations in *PDE6H* and in *KCNV2* have been described in CDSRR. A combined clinical and genetic study was conducted in a cohort of patients with CDSRR, to substantiate these prior results.

Methods. Seventeen patients from 13 families underwent a detailed ophthalmic examination including color vision testing, Goldmann visual fields, fundus photography, Ganzfeld and multifocal ERGs, and optical coherence tomography. The coding sequences and flanking intron/UTR sequences of *PDE6C* and *KCNV2* were screened for mutations by means of DHPLC and direct DNA sequencing of PCR-amplified genomic DNA.

Results. Whereas no mutations were detected in the *PDE6H* gene, mutations in *KCNV2* were identified in all patients, in either the homozygous or compound heterozygous state. Ten of the 11 identified mutations were novel, including three missense and six truncating mutations and one gross deletion. The mutations concordantly segregate in all available families according a recessive mode of inheritance. The CDSRR phenotype was associated with reduced visual acuity of variable degree and color vision defects. Macular defects ranging from mild pigmentary changes to distinct foveal atrophy were present in nine patients. Progression of the disease was observed in only three of seven patients with follow-up data.

Conclusions. The phenotype of cone dystrophy with supernormal rod response is tightly linked with mutations in *KCNV2*. (*Invest Ophthalmol Vis Sci.* 2008;49:751–757) DOI:10.1167/iovs.07-0471

From the [1]Molecular Genetics Laboratory, Institute for Ophthalmic Research, Centre for Ophthalmology, University Clinics Tübingen, Germany; the [2]University Eye Hospital, Centre for Ophthalmology, University Clinics Tübingen, Germany; [3]The Wilhelm Johannsen Centre for Functional Genome Research, Department of Cellular and Molecular Medicine, University of Copenhagen, Denmark; the [4]University Eye Hospital, Munich, Germany; the [5]Department of Medical Genetics, Institute for Human Genetics, University Tübingen, Germany; and the [6]Gordon Norrie Centre for Genetic Eye Diseases, Kennedy Institute–National Eye Clinic, Hellerup, Denmark.

Supported by Grants KFO134: Ko2176/1-1, Ja997/8-1, and Zr1/17-1 from Deutsche Forschungsgemeinschaft.

Submitted for publication April 20, 2007; revised September 24, 2007; accepted December 12, 2007.

Disclosure: **B. Wissinger**, None; **S. Dangel**, None; **H. Jägle**, None; **L. Hansen**, None; **B. Baumann** , None; **G. Rudolph** , None; **C. Wolf**, None; **M. Bonin**, None; **K. Koeppen**, None; **T. Ladewig**, None; **S. Kohl**, None; **E. Zrenner**, None; **T. Rosenberg**, None

The publication costs of this article were defrayed in part by page charge payment. This article must therefore be marked "*advertisement*" in accordance with 18 U.S.C. §1734 solely to indicate this fact.

Corresponding author: Bernd Wissinger, Molecular Genetics Laboratory, Centre for Ophthalmology, University Clinics Tübingen, Röntgenweg 11, D-72076 Tübingen, Germany; wissinger@uni-tuebingen.de.

Cone dystrophy with supernormal rod response (CDSRR) is a retinal disorder characterized by reduced visual acuity, abnormal color vision, discrete macular changes, and specific alterations of ERG responses. The latter constitute reduced and delayed cone responses, a reduction and marked delay of rod b-waves at low light intensities but elevated rod b-wave amplitudes at higher light intensities, which is eponymous for this disorder.

Since its initial description in 1983,[1] several subsequent case series have been published with essentially similar clinical findings.[2–7] The pathomechanism of CDSRR has been disputed controversially in the literature. Because of the similarities with electrophysiological recordings in experimental model systems, notably from cat eyes perfused with IBMX, a potent phosphodiesterase inhibitor, it has been suggested that CDSRR may be caused by a defect of cGMP metabolism in photoreceptors.[1,3,8] However, thorough investigations of the ERG responses of patients with CDSRR led Hood et al.[6] to conclude a pathology distal to the outer segment and most likely occurring at the level of the first synapse.

Although the reported case series on CDSRR suggest an autosomal recessive mode of inheritance, the genetic basis of this disorder remained elusive until very lately. A recent report by Piri et al.[9] seemed to nourish the cGMP metabolism hypothesis. They described a patient with CDSRR who carried a nucleotide substitution in the 5′ untranslated sequence of *PDE6H*, encoding the inhibitory γ-subunit of the cone phosphodiesterase. Functional analysis showed that this mutation increases PDE6H synthesis in vitro. However, doubts remained because this result did not match the expected recessive mode of inheritance and because the unaffected father also carried the mutation.

Only recently, Wu et al.[10] applied a whole-genome autozygosity mapping approach in a large inbred sibship that enabled them to map a locus for CDSRR on chromosome 9p24. Subsequent candidate gene analysis in that region led to the identification of mutations in *KCNV2* in that family and in additional independent patients with CDSRR.

Here we report an independent study to evaluate the prior genetic findings, based on a sample of 17 patients with CDSRR from 13 independent families. In addition, we compiled and compared the clinical data of those patients.

Materials and Methods

Subjects and Clinical Examination

The participants in the study were recruited among patients referred to the National Eye Clinic, Hellerup, Denmark, and the University Eye Clinics in Tübingen and Munich, Germany. The Danish subjects were collected during a 20-year period from 1982 to 2002, and underwent clinical examination for diagnostic reasons. Eleven of the participants

TABLE 1. Oligonucleotide Primers and Sequences

Name	Sequence (5′–3′)	Orientation	Anneal. Temp. (°C)
PDE6HEx1_F	GCATCAACCCATGTTCTCCT	Forward	61
PDE6HEx1_R	CCCCAAAGCCCTTCAATTAT	Reverse	
PDE6HEx2_F	GGTCCCCATGACTTGAAAGA	Forward	60
PDE6HEx2_R	CAATTTCCCAAAACAAAAGCA	Reverse	
PDE6HEx3_F	TCCATGTGAGTGACTCCAAAA	Forward	61
PDE6HEx3_R	AAAGGCAGAACTCCAAGTGC	Reverse	
PDE6HEx4a_F	TTCCTGCCTGAAGGGTGTCT	Forward	60
PDE6HEx4a_R	GCTGGTAGGAAAAGGTGGTC	Reverse	
PDE6HEx4b_F	CCAGAGGTTCTGCCACTCTC	Forward	60
PDE6HEx4b_R	TTTCCTGTATGACTGTGCCTTC	Reverse	
KCNV2_1F	ATCCATCCTCCTAGAGGCAGTGAG	Forward	62
KCNV2_1R	GCTTCTCCATGAGGTTCCAGAGG	Reverse	
KCNV2_2F	CTTCCTGGAGGAGCTGGGCTA	Forward	62
KCNV2_2R	GAAGACGAGGATCAGAAGCCAAAG	Reverse	
KCNV2_3F	TCAGCCAAAGTCTTTCAGCTCCAT	Forward	65
KCNV2_3R	ACATTTCCTTTTGCTGCCAATCAT	Reverse	
KCNV2_TQF	TACGAGGAGCAGACAGACGA	Forward	60
KCNV2-TQR	CCCGGACAGGTAGAAATTGT	Reverse	
KCNV2-TQ	FAM-ACTTCTTCGACCGCGACCCG-BHQ1*	*Taq*man probe	
V2_STR_Fw	TGTGTGCACCTTCTGATTTG	Forward	56
V2_STR_Rv	TCCTGGTTGCTTCTGTCAAG	Reverse	

*FAM, 6-carboxyfluoresceine; BHQ1, black hole quencher 1.

were of Danish descent, one was German, another four were children of a consanguineous couple of Iranian origin, and one was a Caucasian born in Russia. Four of the Danish patients were described in a previous report by Rosenberg and Simonsen.[5]

Patients underwent a standard ophthalmic examination, including evaluation of eye movements, visual acuity (VA), refraction, slit lamp, and fundus examination including fundus photography. Photopic visual field measurements were performed with a Goldmann perimeter (Haag-Streit AG, Bern, Switzerland) using objects I/4e and IV/4e. Color vision screening was performed with Ishihara 38 plates edition 1986, Farnsworth-Munsell D-15 standard and desaturated, Lanthony's Tritan album (LTA), American Optical Hand-Hardy-Rittler (AOHRR), and Nagel's anomaloscope (Schmidt-Haensch, Berlin) were used to classify the anomaly.

Dark adaptation was measured with a Goldmann-Weeker's instrument (Haag-Streit AG) according to the instruction manual for the integral examination of the whole retina or with the Tübingen Hand Perimeter at 20° eccentricity of the nasal hemifield.

Full-field ERG and multifocal ERG recordings were performed in accordance with the ISCEV recommendations. Optical coherence tomography (OCT) scans were obtained with a Stratus OCT (Carl Zeiss Meditec AG, Jena, Germany). Statistical calculations of mean VAs and confidence intervals (CI) were performed with log(VA) to achieve a perceptual metric.

Patients with CDSRR recruited for this study were selected based on pathognomonic ERG findings including (1) reduced b-wave amplitudes and prolonged implicit times in dark-adapted ERG recordings with low-intensity flashes, (2) elevated b-wave amplitudes and prolonged implicit times in dark-adapted ERG recordings with high-intensity flashes, and (3) reduced amplitudes and prolonged implicit time in single-flash light-adapted and/or flicker ERG recordings.

The study was performed according to the tenets of the Declaration of Helsinki, and all participants gave written consent.

Molecular Genetic Analysis

DNA was isolated from peripheral blood according to standard procedures. DNA fragments were amplified from genomic DNA by means of PCR. PCR fragments covering exons 1 to 4 and flanking intron and UTR sequences of *PDE6H* (see Table 1 for primer sequences) were analyzed by denaturing high-performance liquid chromatography (WAVE 3500HT system; Transgenomic Inc., Omaha, NE). The resulting trace profiles were examined with proprietary software (Navigator program; Transgenomics) and compared with the profile of wild-type DNA fragments. Samples with aberrant profiles were sequenced as follows: PCR fragments were subjected to a clean-up protocol (ExoSAP-IT; GE Healthcare, Freiburg, Germany) and then to direct DNA sequencing with dye-termination chemistry (BigDye Terminator ver. 1.1; Applied Biosystems [ABI], Darmstadt, Germany). All sequences were run on a capillary sequencer (ABI 3100; ABI) and analyzed with proprietary sequence trace analysis (Sequence Analysis, ver. 5.1; ABI) or sequence trace alignment software (SeqMan; DNASTAR, Madison, WI).

Mutation screening of the *KCNV2* gene was performed by complete DNA sequencing of the two coding exons and flanking intron and UTR sequences (see Table 1 for primer sequences). Segregation analysis was performed by either DNA sequencing or PCR/RFLP analysis in the presence of diagnostic restriction sites and screening of controls was done by DNA sequencing.

Genotyping of the V2_STR marker (Table 1) was performed by PCR amplification followed by separation on a 12% nondenaturing PAA gel and silver staining.[11]

Quantitative analysis of *KCNV2* DNA copy number was done by real-time PCR employing *Taq*Man technology. Primers KCNV2_TQF and KCNV2-TQR were used to amplify an 81-bp fragment (corresponding to c.424—c.504) of exon 1 of the *KCNV2* gene and real-time quantitative analysis was done by inclusion of a self designed *Taq*Man probe KCNV2-TQ (see Table 1 for oligonucleotide sequences). 25 μL reactions containing 12.5 μL 2x Master Mix (*Taq*Man Universal Master Mix; ABI), 900 nM of each PCR primer, 250 nM of the KCNV2-TQ probe, and 10 ng of genomic DNA were amplified applying the recommended cycling program with 2 min at 50°C, 10 min at 95°C and 40 cycles of 15 s at 95°C and 1 min at 60°C on a real-time PCR cycler (ABI 7500 instrument). In parallel, we performed real-time PCR reactions for a human genome single-copy reference sequence (*Taq*Man RNase P Control Reagent Kit; ABI). Real-time PCRs were performed in triplicate and mean Ct was used for the calculations. The mean of the ΔCt ($Ct_{KCNV2} - Ct_{RNaseP}$) of four control samples were used as calibrator and ΔΔCt and $2^{-\Delta\Delta Ct}$ were calculated for the samples to be assessed.

RESULTS

Screening of the *PDE6H* Gene

A mutation in the 5′ untranslated region (UTR) of *PDE6H* in two siblings with CDSRR has lately been described by Piri et al.[9] To evaluate this finding, we screened all four exons of the *PDE6H* gene, including the 5′ UTR in 13 of our patients with CDSRR by means of DHPLC and DNA sequencing. Six of our 13 patients were heterozygous for a common SNP (rs11056264 in dbSNP) in the 5′ UTR, 59 bp upstream of the annotated start codon, but no other sequence changes were detected in *PDE6H*.

Screening of the *KCNV2* Gene

Wu et al.[10] recently reported mutations in *KCNV2* in patients with CDSRR. We therefore sequenced the whole coding sequence and flanking intron and UTR sequences of the *KCNV2* gene in all 13 index patients of our sample. We were able to identify either homozygous or two heterozygous mutations in every patient. These mutations include five nonsense mutations (p.E73X, p.Q76X, p.E148X, p.K260X, and p.Q287X), a 9-bp in-frame deletion (p.D339_V341del), a gross deletion of parts of the *KCNV2* gene, a 1-bp insertion that results in a frameshift and premature translation termination (p.K120fsX371), and three missense mutations (p.E184K, p.E184V, and p.G461R) (Table 2). The latter were found to be evolutionary highly conserved in KCNV2 channels of various species as well as in the whole family of six transmembrane helices Kv channels. Both the SIFT (provided by the Fred Hutchinson Cancer Research Center, Seattle, WA)[12] and Polyphen (provided by the Division of Genetics, Brigham and Women's Hospital, Harvard Medical School, Boston, MA)[13] programs predicted these substitutions to be deleterious for protein function. Except for the 9-bp in-frame deletion that has been reported by Wu et al.,[10] all other mutations were new. All new point mutations were excluded in >100 (n = 105–115) independent normal Danish control subjects. Cosegregation analysis was performed in 11 families comprising 30 family members. In two families, there was one additional affected sibling, and in one family there were another three affected family members. In all three families, we were able to confirm that the affected siblings share the same two mutant alleles. In contrast, none of the available unaffected siblings (n = 6) showed the same allele combination as their affected sib.

TABLE 2. Mutations in the *KCNV2* Gene

Location	Alteration Nucleotide Sequence*	Alteration Polypeptide	Total Number of Chromosomes‡
Exon 1	c.217G>T	p.E73X	1
Exon 1	c.226C>T	p.Q76X	2
Exon 1	c.357_358insC	p.K120fsX371	5
Exon 1	c.442G>T	p.E148X	5
Exon 1	c.550G>A	p.E184K	1
Exon 1	c.551A>T	p.E184V	1
Exon 1	c.778A>T	p.K260X	1
Exon 1	c.859C>T	p.Q287X	1
Exon 1	c.1016_1024del	p.D339_V341del†	2
Exon 2	c.1381G>A	p.G461R	6
ND	Gross Deletion	ND	1

ND, not determined.

*Reference Sequence: NM_133497. Numbering denotes the adenosine of the annotated translation start codon as nucleotide position 1.

†Mutation reported by Wu et al.[10]

‡Chromosomes counted only for the index patients. Homozygous mutations counted as two chromosomes.

TABLE 3. Real-Time PCR for Dosage Analysis of *KCNV2* Exon 1 Sequences

Subject	Sample No.	ΔCt*	ΔΔCt*	$2^{-\Delta\Delta Ct}$
PWS	14594	0.46	1.03	0.49
Father	16271†	0.60	1.16	0.45
	16402†	0.58	1.15	0.45
Mother	16274	−0.83	−0.26	1.20
Control 1	10565	−0.69		
Control 2	10016	−0.41		
Control 3	16318	−0.49		
Control 4	CEPH	−0.68		

*$\Delta Ct = Ct_{KCNV2} - Ct_{RNaseP}$; $\Delta\Delta Ct = \Delta Ct_{subject} - 1/n \sum_{k=1}^{n} \Delta Ct_{control(k)}$.

†Two independent samples were taken and analyzed.

Based on the sequencing results, patient PWS was initially supposed to be homozygous for the K120fsX371 mutation. However, we failed to detect this mutation in heterozygous state in a blood sample of the father. Because typing of a panel of STR markers ruled out nonpaternity, we reasoned the presence of a heterozygous gross deletion that extends beyond the binding sites of the primers (corresponding to c.1–84_c.1–61 and c.735_c.757) used for the amplification of the basic PCR product. We developed *Taq*Man real-time PCR assay to assess the DNA copy number of exon 1 of *KCNV2* and used an established assay for the single copy gene *RPPH1* on chromosome 14 (*Taq*Man RNase P Control Reagent Kit; ABI) as reference. In comparison with four external controls and the DNA sample of the mother, we found that the sample of PWS and two independent samples of his father exhibited a reduced gene dosage of *KCNV2* (Table 3), thus supporting the presence of a heterozygous deletion. Patient and father were both (apparently) homozygous and identical in sequence for the whole coding sequence of *KCNV2*, hampering a refinement of the deletion by this means. Yet we found that patient PWS was heterozygous for a CA-repeat sequence (V2-STR) located 13.7 kb upstream of *KCNV2* thus defining the outer telomeric border of the deletion.

In addition to the mutations already mentioned, we observed two frequent (c.183C>G/p.Gly61Gly; c.795C>G/p.Ala265Ala) substitutions and one rare silent substitution (c.849G>A/p.Glu283Glu) in the coding sequence of KCNV2.

Clinical Findings in Patients with *KCNV2* Mutations

The clinical data of 16 patients (13 index patients and 3 affected siblings) are summarized in Table 4. The age at examination varied between 2 and 61 years and the observation period from 0 to 24 years. All patients showed ERGs typical of CDSRR (see the Material and Methods section and Fig. 1). Multifocal ERG recordings obtained from patient SR exhibited a loss of responses in the center, whereas more peripheral locations yielded significant responses, yet with reduced amplitudes and prolonged implicit times (Figs. 1B, 1C).

In addition, all subjects had reduced visual acuity (VA) that, in patients for whom earlier data were available, had been noticed from early childhood. Most of the patients had VA in the low-vision interval between 0.4 and 0.2, but acuities in

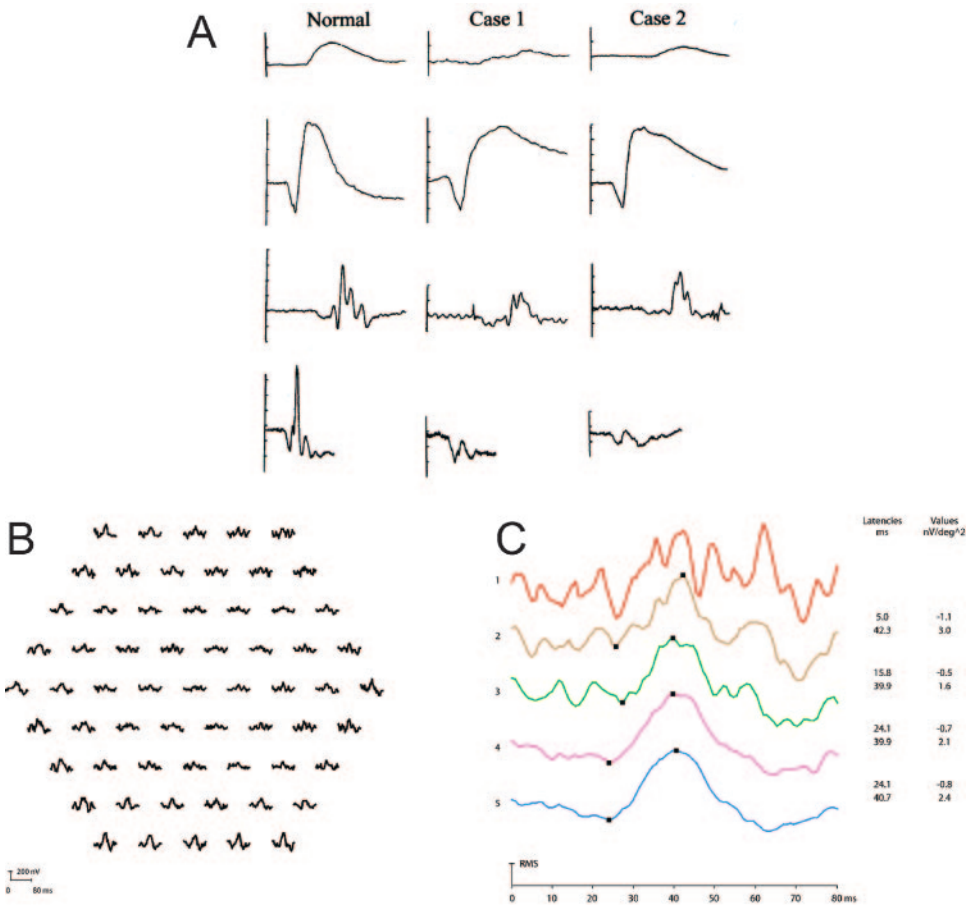

FIGURE 1. Electrophysiological characteristics in cone dystrophy with supernormal rod responses. (**A**) Typical full-field ERG recordings from two affected individuals and a normal control. *Top line*: rod response; *second line*: mixed cone-rod response; *third line*: oscillatory potentials; *bottom line*: light-adapted cone response. Note the attenuated rod response of the affected individuals and a disproportionate exaggerated mixed cone–rod response, both of which exhibit prolonged implicit times. The cone responses are severely reduced, and the oscillatory potentials of the affected are malformed. Vertical scaling of rod and cone–rod recordings, 100 μV; OPs, 20 μV; cone recordings, 50 μV for the control and 10 μV for the affected cases. The durations of the horizontal sequences were 240 ms in three recordings (*first three rows*) and 120 ms in one (*bottom row*). The OP recordings are shown with a 40-ms delay. (**B**) Typical array of local ERG responses obtained with the multifocal ERG. While in the center the responses are not different from noise, significant waveform responses can be identified in the more peripheral locations. (**C**) Concentric ring averages of the responses shown in (**B**). *Top*: the center response, *bottom*: the outermost ring. In those averages which show a significant waveform, the amplitude was severely reduced, and the implicit time was prolonged.

both eyes as low as 0.1 and 0.05 indicate that a more serious disability was present in a few individuals. Refractive values showed a wide variation from high myopia to significant hypermetropia. Color vision deficiency was found in all patients in whom tests were performed. The color vision defects were in particular of mixed red–green type and were in four individuals (KH, PHJ, PWS, and EVT) characterized as extreme protanomaly. In one patient (SR) the Rayleigh-matches on the Nagel anomaloscope were similar to those of achromats consistent with strong scotopization. Most patients (11/16) had early, faint horizontal nystagmus, which eventually disappeared in some. Several patients complained of glare problems. Some of the participants had a history of earlier strabismus for which they had undergone surgery. Only a few patients experienced difficulties in the dark and a statement of night blindness was not always confirmed by examination. Dark adaptation was tested in eight persons, of whom five had incomplete night blindness with a shortened initial course and a 1- to 2-log-unit elevation of the final threshold. Macular changes were mostly inconspicuous, varying from discrete accentuation of the foveal reflexes with a fine stippling of the foveal pigment epithelium (Fig. 2A) to slight irregular foveal depigmentation (Figs. 2B, 2C). A more pronounced, circular foveal atrophy was observed in only two individuals (Figs. 2E, 2F). Fundus examination of patient SR revealed a macular RPE defect. Optic coherence tomography of his macula confirmed this finding by showing a marked atrophy of the retinal layers and the RPE. Disease progression in form of a significant decline in VA and the concomitant development of a distinct foveal atrophy was observed in three of seven patients for whom reliable follow-up data were available (Table 4).

DISCUSSION

In this study, we report the genetic and clinical findings in 17 patients with CDSRR from 13 families. An initial screen of 13 patients for mutations in *PDE6H* failed to detect any putative pathogenic mutation. However, subsequent analysis of the *KCNV2* gene revealed clearly pathogenic mutations in all patients. Besides typical electrophysiological features, our patients consistently showed low vision and color vision defects, but otherwise presented rather variable with respect to VA, refractive error, presence of nystagmus, nyctalopia, and fundus changes. Some patients presented with a normal macula, others with variable RPE defects. Several patients who had been followed for several years showed variable disease courses from no or slight progression to a significant deterioration.

Piri et al.[9] recently identified a nucleotide substitution in the 5′ UTR of the *PDE6H* gene in a single CDSRR family that induces an increase in PDE6H expression in vitro. However, the presence of mutations in *PDE6H* as a cause of CDSRR was not replicated in either the study by Wu et al.[10] or in our sample. Therefore we doubt that mutations in *PDE6H* cause CDSRR. Otherwise such mutations must be very rare.

In a recent study, the gene locus for CDSRR has been mapped to 9p24 by means of autozygosity mapping in a large consanguineous family and subsequently mutations in *KCNV2* were identified in this family as well as in several independent patients.[10] Our data confirm these findings and prove that *KCNV2* is the major gene mutated in CDSRR. Notably, we were able to identify *KCNV2* mutations in all our patients. The patients were either homozygous for a *KCNV2* mutation or carried two compound heterozygous mutations. Concordant segregation results were obtained in all 11 families in which

TABLE 4. Phenotypes of Patients with CDSRR

Sample No./Subject	KCNV2 Allele 1	KCNV2 Allele 2	Sex	Age at Exam.* (years)	VA OD OS	Refraction OD OS	Nystagmus	Color Vision Deficiency	Night Blindness	Fundus	Progression
14588_GD	E73X	G461R	M	4, 5	0.3 0.3	+3.50 +3.50	No	Yes	Yes	Normal	ND
14589_CH	E184K	G461R	F	11, 24	0.3 0.4	−13.50–3.00×15° −13.50–3.00×170°	Yes	Yes	Yes	Slight foveal RPE atrophy, myopic parapapill. crescent	No
14590_KH	G461R	G461R	M	15, 18	0.2 0.25	−4.00–5.0×25° −3.50–1.50×50°	Yes	Yes	ND	Normal	No
14591_PHJ	E148X	E148X	M	17, 36	0.12 0.12	−5.25 −5.00	Yes	Yes	No	Slight foveal atrophy	Yes
14592_IM	D339_ V341del	D339_ V341del	M	50	0.1 0.1	+1.50–1.50×135° +2.50–1.00×75°	No	Yes	No	Distinct foveal RPE atrophy	ND
14593_NN†	K120fs	G461R	M	2, 4	0.08 0.05	−5.00 −5.00–1.00×13°	Yes	ND	ND	Normal	ND
15268_CN†	K120fs	G461R	F	3	0.5 0.3	+2.25 +3.25–1.25×15°	No	Yes	ND	Normal	ND
14594_PWS‡	K120fs	Deletion	M	12, 36	0.08 0.03	−5.00–1.0×0° −6.00	Yes	Yes	Yes	Distinct foveal RPE atrophy	Yes
14595_NMT‡	K120fs	K120fs	F	9, 18	0.05 0.05	+0.75–0.25×100° +1.00–0.25×140°	No	Yes	Yes	Distinct foveal RPE atrophy	Yes
14767_SKH‡	K120fs	G461R	M	53, 61	0.125 0.25	+2.00 +2.00–0.75×150°	Yes	Yes	Yes	Subtle foveal pigment irregularity	No
14768_CA	E148X	E184V	M	21	0.4 0.5	+5.50–1.75×0° +6.00–1.50×165°	No	Yes	Yes	Normal	ND
14769_EVT‡	E148X	E148X	F	10, 25	0.4 0.2	+1.75–1.25×145° +1.00–1.25×60°	Yes	Yes	No	Subtle foveal pigment irregularity	No
11323_SR	K260X	Q287X	M	23	0.16 0.16	−2.0–0.5×130° −2.5–1.0×175°	No	Yes	Yes	Foveal RPE atrophy	No
12357_IRN†	Q76X	Q76X	M	18	0.2 0.2	−5.75–0.5×110° −3.25–1.25×55°	Yes	Yes	No	Normal	No
16386_IHN†	Q76X	Q76X	M	28	0.1 0.1	−3.0–1.5×135° −1.25–1.0×10°	Yes	Yes	No	Maculopathy (posterior pole)	No
16450_IHM†	Q76X	Q76X	M	34	0.1 0.08	−13.0 −12.5–0.75×170°	Yes	Yes	No	Diffuse RPE atrophy (posterior pole and peripapillary)	ND

All patients showed ERG responses typical of CDSRR. ND, no data.
*Age at first and last examination.
†Siblings.
‡Patients (PWS, NMT, SKH, EVP) published in Rosenberg et al.[5]

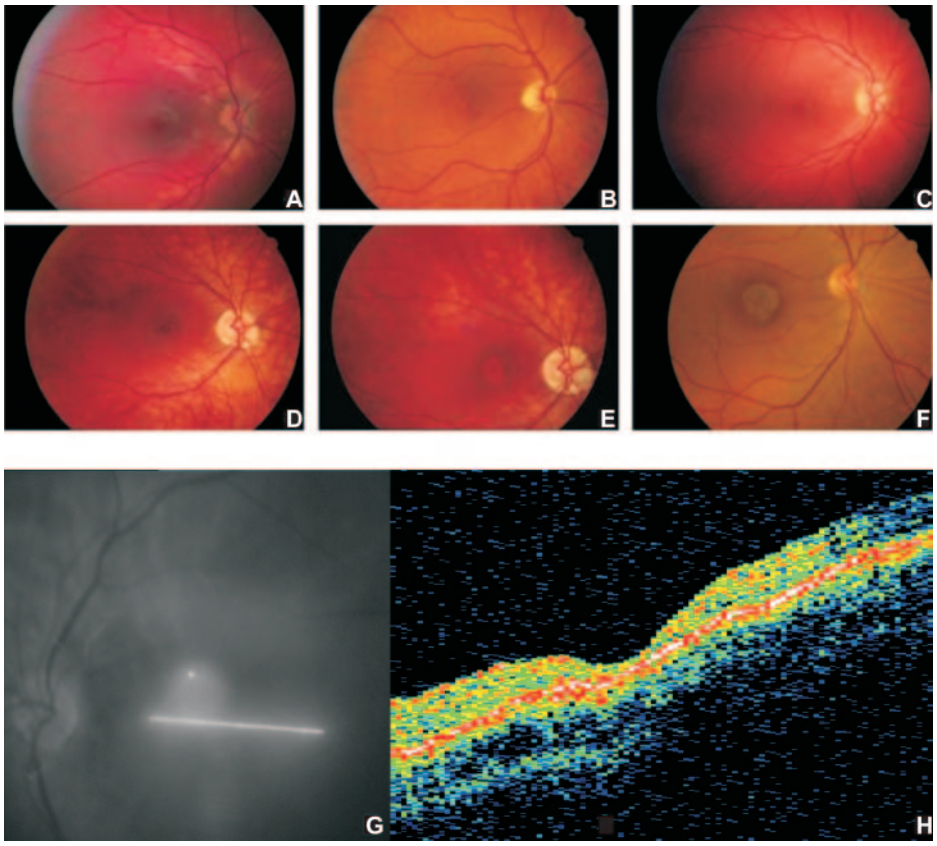

FIGURE 2. Fundus imaging in patients with CDSRR. *Top*: Fundus photographs of five patients. (**A**) Normal fundus of patient GD (age, 5 years). (**B**, **C**) Subtle foveal pigment irregularities in patient SKH (age, 63 years) and patient EVT, (age, 21 years). (**D**, **E**) Progressive foveal depigmentation in patient PWS at the age of 25 and 34 years, respectively. (**F**) Significant, well demarcated, circular foveal pigment epithelial atrophy in patient IM (age, 51 years). *Bottom*: With OCT, the morphologic alterations on patient SR can be illustrated. (**G**) Direction of the OCT scan through the macula. (**H**) The pseudocolored section through the macula shows marked atrophy of retinal layers and the RPE.

samples from additional family members (n = 30) were available. Moreover, all new point mutations were excluded in a representative sample of Danish controls. Six of the identified mutations are either nonsense mutations or cause a translational frameshift that results in truncated or largely altered proteins lacking important functional domains of KCNV2, notably several transmembrane helices and the channel pore. Moreover, those mutant transcripts may undergo nonsense-mediated mRNA decay before actually being translated. Thus these mutations most likely represent functionally *null* alleles in the cellular context. In addition, we identified a gross deletion that includes at least a large proportion of the first of the two exons of *KCNV2*.

Three mutations cause missense substitutions that affect amino acid positions that are highly conserved in evolution and are located in functionally important domains. E184 is located at the outermost position of the N-terminal A- and B-box domain that controls the subfamily-specific tetramerization of heterooligomeric Kv channels.[14] We found E184 to be affected in two distinct mutations that substitute this residue by lysine or valine, respectively, suggesting that E184 represents a functionally very important amino acid at this position. The third missense mutation, G461R, affects the third residue of the ultraconserved -GYG- tripeptide motif that functions as an ion selectivity filter in the pore of Kv channels.[15] Notably, Wu et al.[10] have reported a missense mutation of the first glycine in this very tripeptide.

In our study, we identified altogether 11 different mutations. Ten of these represent new mutations, whereas only the D339_Val341del mutation had been identified in the prior study. The K120fs and the E148X mutations were each present on five mutant alleles and the G461R on six. In total, these three mutations account for more than 60% of all mutant alleles in our patients. The absence of these mutations in the mixed sample of Wu et al.[10] may indicate that they represent founder mutations in the Danish population to which most of the patients belonged.

The clinical data are in accordance with earlier descriptions of the disease.[1–7] The clinical symptoms are rather unremarkable, and unless ERG examinations are routinely applied to cases with a moderate unexplained visual deficiency, the diagnosis will pass unnoticed. The relatively few cases published worldwide compared with the relative high number of diagnosed cases in the small Danish population (5.5 million inhabitants) may indicate that the disorder is widely underdiagnosed. A possible effect from a few Danish founders may also be involved.

Phenotype–genotype correlations were difficult to address because of the allelic heterogeneity and the various allelic combinations in compound heterozygotes. Comparing affected siblings that share identical mutation genotypes, we found a prominent difference in VAs between subjects NN and CN, with NN being one with the worst acuity (0.08/0.05) and CN being one with the best (0.5/0.3). The four affected siblings in family ZD184 who are homozygous for the Q76X mutation (three of them listed in Table 4) had rather uniform VAs that ranged between 0.08 and 0.2. Yet only two of these siblings showed fundus irregularities. It is conceivable that in recessive conditions missense mutations may cause a less severe phenotype than protein-truncating mutations. The missense mutation G461R is the only frequent missense mutation in our sample that is amenable for testing such a hypothesis. When correlating VAs of patients with this mutation with VAs of patients carrying two nonsense alleles (stop or frameshift mutations) we found a mean VA of 0.215 (95% CI: 0.14–0.331) in subjects carrying the G461R (12 eyes) in comparison with a mean VA of 0.117 (95% CI: 0.086–0.16) in subjects carrying two nonsense alleles (18 eyes). These data indicate that the G461R missense mutation may in fact be functionally less severe than protein-truncating mutations. We also noted that all progressive cases in our sample were patients carrying protein-truncating mutations: one patient homozygous for the mutation E148X and

two unrelated patients homozygous for K120fs. Nonetheless, larger patient series and follow-up studies are needed to substantiate this observation.

KCNV2 encodes a modulatory, electrophysiologically silent subunit of the family of voltage-gated potassium channels now called Kv8.2.[16] In vitro Kv8.2 is able to assemble functional heterotetramers with primary potassium channel subunits such as Kv2.1 and Kv3.1. Such heteromeric Kv2.1/Kv8.2 channels show slightly altered electrophysiological properties compared with Kv2.1 homomers.[16]

Expression analysis detected highest levels of *KCNV2* transcripts in pancreas and testis and weaker expression in lung, liver, kidney, spleen, thymus, prostate, and ovary.[16] In the context of its association with CDSRR, Wu et al.[10] studied *KCNV2* expression in the human retina and found its expression to be restricted to the outer retina. Preliminary results from an ongoing study applying single-cell PCR experiments in the mouse retina indicate that *KCNV2* is predominantly expressed in rod photoreceptors (Koeppen K, Ladewig T, unpublished data, 2007). The identity of the primary potassium channel subunit expected to assemble with Kv8.2 in photoreceptors still remains to be established. Various studies and our own data showed that, except for *KCNA7*, all genes encoding primary potassium channel subunits from groups A–D are expressed in the retina[17,18] and transcripts for Kv1.2 to 1.6 and Kv3.3 are present in photoreceptor preparations (Koeppen K, Ladewig T, unpublished data, 2007).

Voltage-gated potassium channels have a wide range of functions, including control of duration and frequency of action potentials and the regulation of the resting membrane potential. The latter is probably the predominant function of potassium channels in photoreceptors. It has been reported that voltage-gated potassium channels found in rods limit the amplitude of spike depolarization.[19,20] Conversely, blocking voltage-gated potassium channels, which decreases membrane conductance and increases rod excitability, always induces spontaneous calcium spikes, thus evoking regenerative potentials.[21]

Further research is needed to clarify the actual role of KCNV2 in photoreceptor response and retinal physiology.

Acknowledgments

The authors thank all the patients and family members for participating; Eva Weber and Monika Papke for technical assistance and thorough management of the DNA sample library and the DNA sequencing core, respectively, at the Molecular Genetics Laboratory, University Eye Hospital, Tübingen; and Maria Jörgensen for help with the screening of the Danish control subjects.

References

1. Gouras P, Eggers HM, MacKay CJ. Cone dystrophy, nyctalopia, and supernormal rod responses: a new retinal degeneration. *Arch Ophthalmol*. 1983;101(5):718–724.
2. Alexander KR, Fishman GA. Supernormal scotopic ERG in cone dystrophy. *Br J Ophthalmol*. 1984;68(2):69–78.
3. Sandberg MA, Miller S, Berson EL. Rod electroretinograms in an elevated cyclic guanosine monophosphate-type human retinal degeneration: comparison with retinitis pigmentosa. *Invest Ophthalmol Vis Sci*. 1990;31(11):2283–2287.
4. Kato M, Kobayashi R, Watanabe I. Cone dysfunction and supernormal scotopic electroretinogram with a high-intensity stimulus: a report of three cases. *Doc Ophthalmol*. 1993;84(1):71–81.
5. Rosenberg T, Simonsen SE. Retinal cone dysfunction of supernormal rod ERG type: five new cases. *Acta Ophthalmol* (*Copenh*). 1993;71(2):246–255.
6. Hood DC, Cideciyan AV, Halevy DA, Jacobson SG. Sites of disease action in a retinal dystrophy with supernormal and delayed rod electroretinogram b-waves. *Vision Res*. 1996;36(6):889–901.
7. Michaelides M, Holder GE, Webster AR, et al. A detailed phenotypic study of "cone dystrophy with supernormal rod ERG." *Br J Ophthalmol*. 2005;89(3):332–339.
8. Sandberg MA, Pawlyk BS, Crane WG, Schmidt SY, Berson EL. Effects of IBMX on the ERG of the isolated perfused cat eye. *Vision Res*. 1987;27(9):1421–1430.
9. Piri N, Gao YQ, Danciger M, Mendoza E, Fishman GA, Farber DB. A substitution of G to C in the cone cGMP-phosphodiesterase gamma subunit gene found in a distinctive form of cone dystrophy. *Ophthalmology*. 2005;112(1):159–166.
10. Wu H, Cowing JA, Michaelides M, et al. Mutations in the gene KCNV2 encoding a voltage-gated potassium channel subunit cause "cone dystrophy with supernormal rod electroretinogram" in humans. *Am J Hum Genet*. 2006;79(3):574–579.
11. Bassam BJ, Caetano-Anollés G, Gresshoff PM. Fast and sensitive silver staining of DNA in polyacrylamide gels. *Anal Biochem*. 1991;196(1):80–83.
12. Ng PC, Henikoff S. Predicting the effects of amino Acid substitutions on protein function. *Annu Rev Genomics Hum Genet.* 2006;7:61–80.
13. Sunyaev S, Ramensky V, Koch I, Lathe W 3rd, Kondrashov AS, Bork P. Prediction of deleterious human alleles. *Hum Mol Genet.* 2001;10(6):591–597.
14. Shen NV, Pfaffinger PJ. Molecular recognition and assembly sequences involved in the subfamily-specific assembly of voltage-gated K+ channel subunit proteins. *Neuron*. 1995;14(3):625–633.
15. Heginbotham L, Lu Z, Abramson T, MacKinnon R. Mutations in the K+ channel signature sequence. *Biophys J*. 1994;66(4):1061–1067.
16. Ottschytsch N, Raes A, Van Hoorick D, Snyders DJ. Obligatory heterotetramerization of three previously uncharacterized Kv channel alpha-subunits identified in the human genome. *Proc Natl Acad Sci USA*. 2002;99(12):7986–7991.
17. Pinto LH, Klumpp DJ. Localization of potassium channels in the retina. *Prog Retin Eye Res*. 1998;17(2):207–230.
18. Ozaita A, Petit-Jacques J, Volgyi B, et al. A unique role for Kv3 voltage-gated potassium channels in starburst amacrine cell signaling in mouse retina. *J Neurosci*. 2004;24(33):7335–7343.
19. Attwell D, Wilson M. Behaviour of the rod network in the tiger salamander retina mediated by membrane properties of individual rods. *J Physiol*. 1980;309:287–315.
20. Barnes S. After transduction: response shaping and control of transmission by ion channels of the photoreceptor inner segments. *Neuroscience*. 1994;58(3):447–459.
21. Xu JW, Hou M, Slaughter MM. Photoreceptor encoding of supersaturating light stimuli in salamander retina. *J Physiol*. 2005;569:575–585.